

Cryogenic SIMS preserving elemental distributions formed under extreme conditions: Hydrogen distribution measurement in iron

Naoya Sakamoto¹ | Nagi Ikuta² | Kei Hirose^{2,3} | Shoh Tagawa³ | Koutaro Hikosaka² | Shuhei Mita²

¹Institute for Integrated Innovations, Hokkaido University, Sapporo, Japan

²Department of Earth and Planetary Science, The University of Tokyo, Tokyo, Japan

³Earth-Life Science Institute, Institute of Science Tokyo, Tokyo, Japan

Correspondence: Naoya Sakamoto (naoya@cris.hokudai.ac.jp)

Keywords: SIMS | cryogenic measurements | hydrogen | iron | high pressure

ABSTRACT

We established a cryogenic secondary ion mass spectrometry (Cryo-SIMS) system, in which all procedures—sample recovery, transport, and analysis—are performed under cryogenic temperatures. Using this system, we determined hydrogen concentrations in Fe-H alloys, which form only under high pressure and lose hydrogen upon decompression at ambient temperature. The hydrogen contents obtained were in good agreement with the X-ray diffraction (XRD) measurements conducted under high pressure. The present cryogenic SIMS techniques can be applied to the determination of hydrogen isotopic composition of iron alloys, which is not possible with XRD analysis, but is important for understanding the origin of water on Earth.

1 | Introduction

Secondary ion mass spectrometry (SIMS) is among the few techniques capable of highly sensitive analyses of trace light elements including hydrogen [1]. Early efforts to analyze liquids, such as fluid inclusions, employed a cryogenic sample stage to suppress volatilization under the ultra-high vacuum conditions required for SIMS analyses [2]. However, elemental distributions established under extreme pressure and temperature (P - T) conditions are sometimes not preserved during decompression to ambient pressure for sample recovery. A typical example is an iron-hydrogen alloy: hydrogen escapes from the iron lattice during decompression when the crystal structure changes to body-centered cubic (bcc) at room temperature [3, 4]. The study of metal hydrides is important because hydrogen in metals is known to cause their embrittlement [5–7]. In addition, hydrogen is considered likely to be a major light element impurity of the Earth’s core [4, 8, 9], but its exact composition remains uncertain [10]. The hydrogen isotopic ratio in the core is also unknown.

39

40 Here, we established a workflow to execute all processes after sample synthesis under
41 cryogenic temperatures by developing a Cryo-SIMS system that enables the introduction and
42 analysis of frozen samples in ultra-high vacuum [11–15]. We used this system to examine Fe-
43 H alloys originally synthesized under high P - T conditions in a diamond-anvil cell (DAC). The
44 sample was decompressed and recovered from the DAC in liquid N_2 , then transferred to a SIMS
45 instrument for analysis. The hydrogen contents in iron determined by the SIMS measurements
46 were in good agreement with those estimated by XRD analyses performed under high pressures.
47 The present technique enables three-dimensional quantification of element concentrations and
48 isotopic ratios in a small sample synthesized under extreme P - T conditions relevant to the core
49 and will thus be helpful for understanding the origin and distribution of Earth’s water
50 (hydrogen).

51

52 **2 | Experimental Procedures**

53

54 Iron-hydrogen alloys were synthesized under high P - T in a laser-heated DAC combined with
55 synchrotron XRD measurements [16, 17]. We used a circular Re gasket (3 mm in diameter),
56 preindented it to ~ 40 μm in thickness, and drilled a ~ 100 μm diameter hole at its center to form
57 a sample chamber. A ~ 7 μm thick Fe foil (5N, Mairon-UHP, Toho Zinc Co. Ltd.) was placed
58 between the ~ 10 μm thick KCl layers, which served as both a pressure medium and a thermal
59 insulator, while leaving room for hydrogen. The entire DAC was then dried in a vacuum oven
60 at 400 K for at least 2 hours to eliminate moisture in the sample chamber. Subsequently,
61 supercritical hydrogen fluid was introduced into the sample chamber using a 200 MPa high-
62 pressure gas apparatus (PRETECH Co., Ltd.) at SPring-8 [16, 17]. After compression under
63 room temperature, it was heated from both sides with a pair of 100 W single-mode Yb fiber
64 lasers (IPG Photonics) at the beamline BL10XU, SPring-8. The entire sample was
65 hydrogenated upon heating to < 1000 K for about 30 minutes. Furthermore, we melted the
66 central portion of the Fe-H sample by heating to $2440(\pm 120)$ K at $48(\pm 5)$ GPa for 3 seconds.
67 Temperature was measured using a spectro-radiometric method [18]. Pressure was determined
68 based on the thermal EoS of KCl [19].

69

70 We collected XRD patterns of the sample on a flat panel X-ray detector (Perkin Elmer,
71 XRD0822 CP23) with an incident X-ray beam that was monochromatized to ~ 30 keV and
72 focused to 6 μm in diameter (full-width at half maximum) [18] (Figure 1). Given that the lattice
73 volume of Fe expands proportionally with the hydrogen content [20], the hydrogen
74 concentration, x , in FeH_x was estimated from the XRD data collected at 300 K [4, 16, 17] as:

75

$$x = \frac{V_{\text{FeH}_x} - V_{\text{Fe}}}{\Delta V_{\text{H}}} \quad (1)$$

76 where V_{FeH_x} and V_{Fe} are the volumes per Fe atom for FeH_x determined from the present
77 XRD measurements and for pure Fe from earlier experiments [21], respectively, and ΔV_{H}
78 represents the increase in the lattice volume of Fe caused by the incorporation of an H atom
79 [22]. Upon annealing at <1000 K, the hydrogen content of the sample increased to $x = 0.25$
80 (Figure 1). After heating to 2440 K, we found $x = 0.30(\pm 0.05)$ at the center of the laser-heated
81 hot spot, corresponding to the melted portion consisting of quench crystals with the face-
82 centered cubic (fcc) structure that formed from the liquid upon temperature quenching. The
83 XRD analyses also showed an fcc phase with $x = 0.87(\pm 0.08)$, corresponding to the surrounding
84 unmelted area, where the hydrogen concentration increased due to the higher temperature,
85 which further enhanced hydrogenation.

86

87 The sample was then decompressed in liquid nitrogen to avoid hydrogen loss from the iron.
88 Earlier experiments [23] demonstrated that hydrogen remains in the iron lattice below
89 approximately -70 °C under vacuum. To do this, we first submerged the DAC in liquid nitrogen
90 and waited for several minutes for the temperature to equilibrate. We then fully released
91 pressure, retrieved the rhenium gasket containing the Fe-H sample and KCl, and placed the
92 gasket in an in-house cryo-holder, all while ensuring the sample remained in the liquid nitrogen.
93 It was then placed in a sample carrier also filled with liquid nitrogen and transported to the
94 SIMS instrument at Hokkaido University. The sample temperature was maintained at liquid
95 nitrogen temperature throughout these processes. A valved environmental control airlock was
96 attached to the sample carrier to introduce the sample into the SIMS system. While the carrier
97 was being evacuated, the sample holder was lifted from the liquid nitrogen and stored in the
98 airlock that was filled with evaporated nitrogen gas and sealed off from the outside air. The
99 airlock was then immediately attached to the SIMS system, and the sample was transferred via
100 a storage chamber to a liquid nitrogen-cooled freezing stage (Techno I.S.), where a
101 thermocouple located directly underneath the sample holder monitored the temperature and
102 ensured it stayed below -180 °C. It took approximately 50 seconds to remove the sample from
103 the carrier filled with liquid nitrogen and place it on the freezing stage.

104

105 The Fe-H sample, mounted on a freezing stage, was examined with an isotope microscope
106 system consisting of a stigmatic SIMS instrument (CAMECA ims-1270e7) and a stacked
107 CMOS-type active pixel sensor (SCAPS), which provides quantitative projection images of
108 secondary ions emitted from the sample surface and thus enables quantification of the
109 abundance of each element from the intensity map [24]. The sample surface was irradiated with
110 a 13 keV O^- beam, defocused to approximately 50 μm in diameter (the projection image
111 exhibits submicron lateral spatial resolution, see Figures 2 and 3), at a probe current of 100 nA
112 and a sweep electrode setting of 150×150 μm on the sample surface. Secondary ions sputtered
113 from the sample surface were extracted at 10 keV while preserving their positional information

114 and projected onto the SCAPS detector through an energy offset, contrast aperture, energy slit,
115 and exit slit. Pre-sputtering was conducted until the KCl pressure medium on top of the Fe foil
116 was removed, and analysis was performed once the entire Fe foil was exposed. The isotopes
117 analyzed were $^1\text{H}^+$ and $^{56}\text{Fe}^+$, with net signal acquisition times of 2000 and 5 seconds,
118 respectively. The quantitative images obtained were processed using ImageJ software. The
119 isotope images were appropriately noise-reduced by multi-frame averaging [25], and the line
120 profiles were averaged over 10 pixels.

121

122 **3 | Results**

123

124 [Figure 2a](#) shows a hydrogen image obtained using the developed Cryo-SIMS method.
125 Hydrogen was detected throughout the entire Fe foil (see [Figure 3](#) for the outline of the Fe foil).
126 The gray scale represents the total number of ions detected over the entire acquisition time.
127 The dark (melted) area at the center of the Fe foil corresponds to the portion heated to 2440 K
128 by laser irradiation while the DAC was pressurized to 48 GPa. The XRD peaks from the
129 hexagonal close-packed (hcp) structure disappeared during heating, indicating that this region
130 melted ([Figure 1](#)). The KCl pressure medium remained between the Fe foil and the Re gasket,
131 as well as in the area that was not completely removed by pre-sputtering ([Figure 2a](#)). [Figure 2c](#)
132 shows the line profile of $^1\text{H}^+$ counts, indicating that the hydrogen signal from the melted portion
133 is weak, approximately one-fifth of that for the surrounding area. Hydrogen was also detected
134 from the region of the gasket that was in contact with H_2 , where rhenium was also hydrogenated.
135 We note, however, that such hydrogenation of the gasket was limited to its rim, precluding a
136 remarkable hydrogen loss to the outside of a sample chamber during heating.

137

138 After performing these cryogenic analyses, the sample holder was transferred from the freezing
139 stage to a room-temperature, vacuum storage chamber and left overnight to allow the sample
140 temperature to increase to 300 K. The sample was then returned to the freezing stage, and
141 similar analyses were performed again under cryogenic temperatures. While traces of hydrogen
142 were detected from the hydrogenated Re and water-adsorbed KCl, no hydrogen signal was
143 observed from the Fe foil ([Figure 2b](#)). According to the line profile in [Figure 2d](#) (note that the
144 vertical axis is a linear scale), the hydrogen signal in the Fe foil area was below the noise level,
145 indicating that the hydrogen in the Fe had almost completely been lost upon increasing
146 temperature to room temperature.

147

148 [Figure 3](#) provides the Cryo-SIMS images for Fe before and after raising sample temperature to
149 300 K, and their respective line profiles. Under cryogenic conditions, the Fe signal from the
150 melted area was lower than in the surrounding area, just like the H signal, but the difference
151 was minor compared to H. We also note that the Fe signal was reduced after increasing the

152 temperature to room temperature, particularly in the surrounding unmelted portion. There was
153 almost no difference in signal between the central melted area and its surroundings at room
154 temperature.

155
156 Finally, we compare the H/Fe count ratios obtained by Cryo-SIMS with the H/Fe molar ratios
157 (equivalent to x in FeH_x) determined from the XRD data in [Figure 4](#). When considering their
158 uncertainties, the correlation line between the data for H-poor melted and H-rich surrounding
159 areas ($x = 0.30 \pm 0.05$ and 0.87 ± 0.08 , respectively, from the XRD data) goes to the origin of the
160 coordinate system, indicating that these SIMS and XRD measurements are in good agreement
161 with each other.

162

163 **4 | Discussion**

164

165 Hydrogen was detected from an Fe foil that was hydrogenated at high pressure and kept at low
166 temperatures throughout the subsequent procedures, from decompression in liquid nitrogen to
167 analyses on a cryo-stage in the SIMS instrument ([Figure 2a](#)). In contrast, hydrogen was no
168 longer observed once the temperature of the Fe foil was increased to room temperature
169 overnight in a vacuum and then analyzed again under the same cryogenic conditions ([Figure](#)
170 [2b](#)). This clearly demonstrates that temperature is related to the behavior of hydrogen. Indeed,
171 it has been shown that FeH rapidly loses hydrogen when it reaches about $-70\text{ }^\circ\text{C}$ in a vacuum
172 [23], indicating that the loss of the hydrogen signal in SIMS was certainly due to hydrogen
173 escape when the sample temperature was increased. This dictates that successful SIMS analysis
174 of hydrogen in iron requires maintaining the sample temperature below $-70\text{ }^\circ\text{C}$ [23] throughout
175 the entire process, from sample recovery to ion beam irradiation. The detection of hydrogen in
176 iron in this study demonstrates that the developed Cryo-SIMS system enables cryogenic
177 analysis by maintaining temperatures below $-70\text{ }^\circ\text{C}$.

178

179 While SIMS is a highly sensitive in-situ analytical method, a matrix effect is known, in which
180 the signal intensity obtained varies depending on the crystal structure and composition of the
181 target [26]. We note that both the H and Fe signal intensities obtained by Cryo-SIMS were
182 lower in the melted area at the center of the Fe-H sample than in the surrounding unmelted
183 portion ([Figures 2a, 3a](#)). It indicates a compositionally derived matrix effect, since Fe-H alloys
184 in both melted and unmelted areas should have adopted the fcc crystal structure until hydrogen
185 was released from iron (the fcc structure observed by high-pressure XRD data for both melted
186 and unmelted parts should have been preserved after pressure release under cryogenic
187 temperatures). Moreover, the Fe intensity from hydrogen-lost pure Fe foil acquired after the
188 sample temperature was raised to room temperature was overall lower ([Figure 3b](#)) than that
189 from Fe-H alloys ([Figure 3a](#)). It is consistent with the observation described above—the lower

190 the hydrogen counts, the lower the iron counts (Figures 2a, 3a)—although it may be due to a
191 slight difference in the primary ion beam intensity or a difference in crystal structure (bcc is
192 the stable structure at 300 K). Because of such a matrix effect, the three-fold difference in the
193 H/Fe molar ratio (Figure 4) caused the five-fold difference in hydrogen counts from iron
194 between the melted and surrounding unmelted portions (Figure 2a). While these H and Fe
195 analyses were performed after the KCl layer on top of the Fe foil was removed by pre-sputtering,
196 we obtained only the background level of potassium in the secondary ion image of $^{39}\text{K}^+$ for the
197 Fe-H sample, indicating that the effect of potassium contamination was negligible.

198
199 The H/Fe ratios of the molten and unmolten regions obtained by XRD and SIMS analyses are
200 plotted on a single straight line passing through the origin of the coordinate system (Figure 4),
201 indicating the potential for use as a calibration curve for the SIMS determinations of hydrogen
202 in iron without XRD data. The Cryo-SIMS techniques developed in this study enable highly
203 sensitive quantification of the hydrogen isotope ratio and concentration with submicron-scale
204 lateral spatial resolution and nanometer-scale depth resolution, while maintaining its
205 distributions formed in extreme high-pressure and -temperature environments relevant to
206 planetary interiors. The presence of a large amount of hydrogen in the Earth's core has been
207 supported by various aspects, such as its siderophile (iron-loving) nature [4] and compatibility
208 of the density and velocity of liquid Fe-H with seismological observations of the outer core
209 [27]. A combination of high-pressure melting experiments and Cryo-SIMS measurements is
210 expected to reveal hydrogen isotopic fractionation between the silicate mantle and the metallic
211 iron core, which gives the bulk Earth hydrogen isotopic ratio constraining the origins of Earth's
212 water (hydrogen).

213
214 Samples retrieved from high pressures are usually handled at ambient pressure and temperature
215 under atmospheric air. However, samples synthesized under high P - T often change their crystal
216 structure when the pressure is released at room temperature, and, as demonstrated here,
217 sometimes change their chemical composition (e.g., lose hydrogen). We applied our newly
218 developed Cryo-SIMS techniques to the high P - T sample and successfully determined
219 hydrogen concentrations in Fe-H alloys before hydrogen escapes from iron above $-70\text{ }^\circ\text{C}$ [23].
220 This Cryo-SIMS method will also contribute to the characterization of living organisms, which
221 are mostly composed of water that evaporates in the ultra-high vacuum of a SIMS instrument
222 and therefore cannot be analyzed unless at cryogenic temperatures. This new method enables
223 isotope analysis of water in the brain or vacuoles in plants. Samples from space may also
224 require the present techniques, which involve sample recovery and transfer in liquid N_2 and
225 high vacuum environments under cryogenic temperatures, thereby helping to avoid
226 contamination and alteration by air.

227

228 **5 | Conclusion**

229

230 We established a fully cryogenic SIMS workflow (Cryo-SIMS), in which all processes,
231 including sample preparation, transfer, and analysis, are performed under cryogenic conditions
232 using liquid nitrogen. This suppresses atomic and molecular mobility and therefore effectively
233 prevents elemental redistribution, preserving the original elemental and isotopic
234 distributions. Here, we applied such Cryo-SIMS techniques to the quantification of hydrogen
235 concentration in Fe-H alloys, which form only under high *P-T* conditions and lose hydrogen
236 when samples are recovered at ambient temperature. The Cryo-SIMS analyses showed the
237 hydrogen contents in iron, in good agreement with synchrotron XRD measurements performed
238 under high pressure. The method developed in this study will also be useful for investigating
239 biological samples and those retrieved from space by sample return missions.

240

241

242 **Author Contributions**

243 **Naoya Sakamoto:** conceptualization (equal), methodology (equal), investigation (equal),
244 formal analysis (equal), resources (equal), funding acquisition (equal), writing – original draft
245 (equal). **Nagi Ikuta:** investigation (equal), formal analysis (equal), writing – original draft
246 (equal). **Kei Hirose:** methodology (equal), funding acquisition (equal), writing – original draft
247 (equal). **Shoh Tagawa:** investigation (equal). **Koutaro Hikosaka:** investigation (equal).
248 **Shuhei Mita:** investigation (equal).

249

250 **Acknowledgements**

251 We thank two anonymous reviewers for their valuable comments, which helped improve the
252 manuscript. XRD measurements were carried out on the BL10XU beamline at SPring-8 under
253 the approval with JASRI (proposal nos. 2023B1697 and 2024A1157). We also thank N. Hirao,
254 S-I. Kawaguchi, H. Kadobayashi, and K. Oka for their help in high-pressure gas loading and
255 XRD measurements.

256

257 **Funding**

258 This work was supported by JST FOREST (grant no. JPMJFR2173) to N.S. and JSPS
259 KAKENHI (grants no. 21H04968 and 26H02080) to K.H.

260

261 **Conflicts of Interest**

262 The authors declare no conflicts of interest.

263

264 **Data Availability Statement**

265 The data that support the findings of this work will be available upon reasonable requests.

266

267 **References**

268

269 1. J. P. Greenwood, S. Itoh, N. Sakamoto, P. Warren, L. Taylor, and H. Yurimoto, “Hydrogen
270 Isotope Ratios in Lunar Rocks Indicate Delivery of Cometary Water to the Moon,”

271 *Nature Geoscience* 4 (2011): 79–82.

272 2. T. Sato, M. Nambu, Y. Omori, and N. Hayakawa, “On the Analysis of Fluid Inclusion on
273 Quartz with Ion Micro Analyzer,” *Bulletin of the Research Institute of Mineral Dressing and*
274 *Metallurgy, Tohoku University* 33 (1978): 92–102. (in Japanese)

275 3. R. Iizuka-Oku, T. Yagi, H. Gotou, T. Okuchi, T. Hattori, and A. Sano-Furukawa,
276 “Hydrogenation of Iron in the Early Stage of Earth’s Evolution,” *Nature Communications* 8
277 (2017): 14096.

278 4. S. Tagawa, N. Sakamoto, K. Hirose, S. Yokoo, J. Hernlund, Y. Ohishi, and H. Yurimoto,
279 “Experimental Evidence for Hydrogen Incorporation into Earth’s Core,” *Nature*
280 *Communications* 12 (2021): 2588.

281 5. H. Yu, A. Díaz, X. Lu, B. Sun, Y. Ding, M. Koyama, J. He, X. Zhou, A. Oudriss, X. Feaugas,
282 and Z. Zhang, “Hydrogen Embrittlement as a Conspicuous Material Challenge—
283 Comprehensive Review and Future Directions,” *Chemical Reviews* 124 (2024): 6271.

284 6. J. Song, and W. Curtin, “Atomic Mechanism and Prediction of Hydrogen Embrittlement in
285 Iron,” *Nature Materials* 12 (2013): 145.

286 7. V. Madina, and I. Azkarate, “Compatibility of Materials with Hydrogen. Particular Case:
287 Hydrogen Embrittlement of Titanium Alloys,” *International Journal of Hydrogen Energy* 34
288 (2009): 5976.

289 8. T. Okuchi, “Hydrogen Partitioning into Molten Iron at High Pressure: Implications for
290 Earth’s Core,” *Science* 278 (1997): 1781.

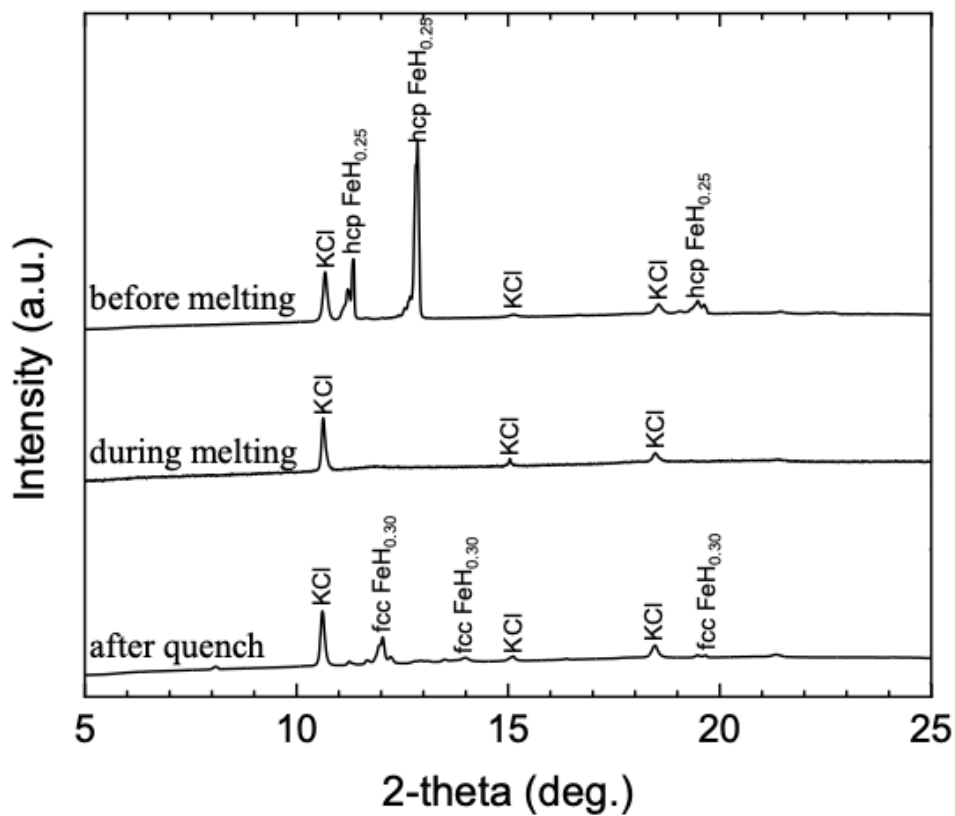
291 9. L. Yuan, and G. Steinle-Neumann, “Strong Sequestration of Hydrogen into the Earth’s Core
292 During Planetary Differentiation,” *Geophysical Research Letters* 47 (2020): e2020GL088303

293 10. K. Hirose, B. Wood, and L. Vočadlo, “Light Elements in the Earth’s Core,” *Nature Reviews*
294 *Earth & Environment* 2 (2021): 645–658.

295 11. T. Suzuki, “Cryogenic TOF-SIMS Around Sublimation Temperature of Quench-
296 Condensed Noble Gas (Ne, Ar, and Kr) Films,” *Journal of Mass Spectrometry* 60 (2025):
297 e5107.

- 298 12. C. Seydoux, B. Moreau, M. Boujard, E. Gautier, P. Jouneau, and J. Barnes, “In Situ GCIB
299 Cryo-Sectioning Enables Subcellular Cryo-ToF-SIMS Imaging of Arabidopsis Seeds,”
300 *Journal of the American Society for Mass Spectrometry* (2026): doi:10.1021/jasms.5c00420
- 301 13. R. Metzner, H. Schneider, U. Breuer, M. Thorpe, U. Schurr, W. Schroeder, “Tracing
302 Cationic Nutrients from Xylem into Stem Tissue of French Bean by Stable Isotope Tracers and
303 Cryo-Secondary Ion Mass Spectrometry,” *Plant Physiology* 152 (2010): 1030.
- 304 14. P. Jovičević-Klug, N. Lipovšek, M. Jovičević-Klug, M. Mrak, J. Ekar, B. Ambrožič, G.
305 Dražić, J. Kovač, and B. Podgornik, “Assessment of Deep Cryogenic Heat-Treatment Impact
306 on the Microstructure and Surface Chemistry of Austenitic Stainless Steel,” *Surfaces and*
307 *Interfaces* 35 (2022): 102456.
- 308 15. M. Dickinson, P. Heard, J. Barker, A. Lewis, D. Mallard, and G. Allen, “Dynamic SIMS
309 Analysis of Cryo-Prepared Biological and Geological Specimens,” *Applied Surface Science*
310 252 (2006): 6793.
- 311 16. S. Mita, S. Tagawa, K. Hirose, and N. Ikuta, “Fe-FeH Eutectic Melting Curve and the
312 Estimates of Earth’s Core Temperature and Composition,” *Journal of Geophysical Research:*
313 *Solid Earth* 130 (2025): e2024JB029283.
- 314 17. S. Fu, K. Hirose, S. Yokoo, F. Sakai, and K. Oka, “Hydrogen in the Earth’s Outer Core
315 from Density Measurements of Liquid Fe-H up to 102 GPa and 4,100 K,” *Journal of*
316 *Geophysical Research: Solid Earth* 130 (2025): e2025JB031934.
- 317 18. N. Hirao, S. I. Kawaguchi, K. Hirose, K. Shimizu, E. Ohtani, and Y. Ohishi, “New
318 Developments in High-pressure X-ray Diffraction Beamline for Diamond Anvil Cell at SPring-
319 8,” *Matter and Radiation Extremes* 5 (2020): 018403.
- 320 19. S. Tateno, T. Komabayashi, K. Hirose, N. Hirao, and Y. Ohishi, “Static Compression of
321 B2 KCl to 230 GPa and Its *P-V-T* Equation of State,” *American Mineralogist* 104 (2019): 718–
322 723.
- 323 20. R. Caracas, “The Influence of Hydrogen on the Seismic Properties of Solid Iron,”
324 *Geophysical Research Letters* 42 (2015): 3780–3785.
- 325 21. P. I. Dorogokupets, A. M. Dymshits, K. D. Litasov, and T. S. Sokolova, “Thermodynamics
326 and Equations of State of Iron to 350 GPa and 6000 K,” *Scientific Reports* 7 (2017): 41863.
- 327 22. S. Tagawa, H. Gomi, K. Hirose, and Y. Ohishi, “High-temperature Equation of State of
328 FeH: Implications for Hydrogen in Earth’s Inner Core,” *Geophysical Research Letters* 49
329 (2022): e2021GL096260.

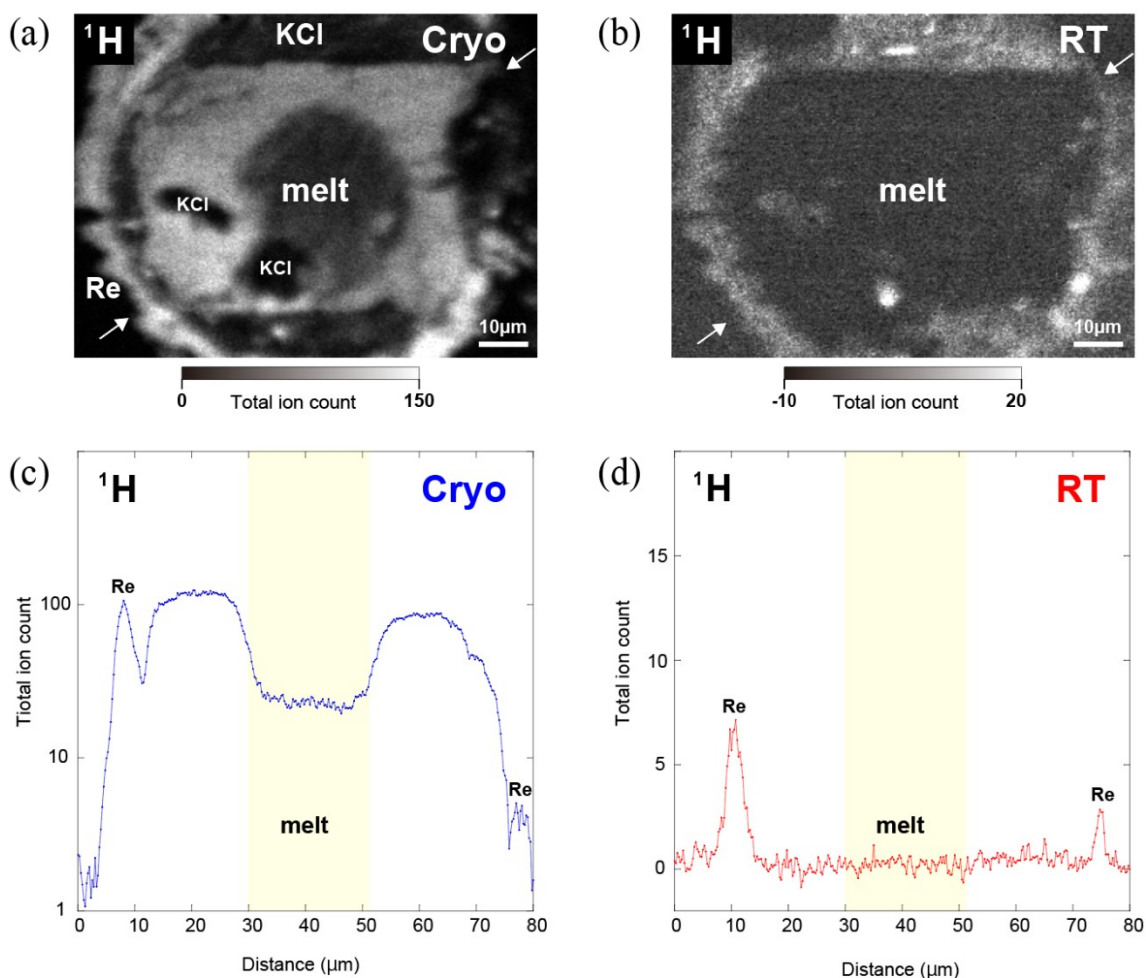
- 330 23. V. E. Antonov, V. M. Gurev, V. I. Kulakov, M. A. Kuzovnikov, I. A. Sholin, and V. Y.
331 Zuykova, “Solubility of Deuterium and Hydrogen in Fcc Iron at High Pressures and
332 Temperatures,” *Physical Review Materials* 3 (2019): 113604.
- 333 24. H. Yurimoto, K. Nagashima, and T. Kunihiro, “High Precision Isotope Micro-imaging of
334 Materials,” *Applied Surface Science* 203-204 (2003): 793–797.
- 335 25. K. Yamamoto, N. Sakamoto, and H. Yurimoto, “Analysis of the Noise Properties of a
336 Solid-state SCAPS Ion Imager and Development of Software Noise Reduction,” *Surface and*
337 *Interface Analysis* 42 (2010): 1603–1605.
- 338 26. A. Benninghoven, F. G. Rudenauer, and H. W. Werner, “Secondary Ion Mass Spectrometry;
339 Basic Concepts, Instrumental Aspects, Applications and Trends,” *Chemical analysis*, Vol. 86
340 (Wiley, New York 1987).
- 341 27. K. Umemoto and K. Hirose, “Chemical Compositions of the Outer Core Examined by First
342 Principles Calculations,” *Earth and Planetary Science Letters* 531 (2020): 116009.
343



345

346 **FIGURE 1** | XRD patterns obtained at 48 GPa before/during/after melting the Fe + H₂ sample.347 Loss of the peaks from hcp FeH_{0.25} indicates melting. Fcc FeH_{0.30} formed from liquid upon
348 quenching the temperature.

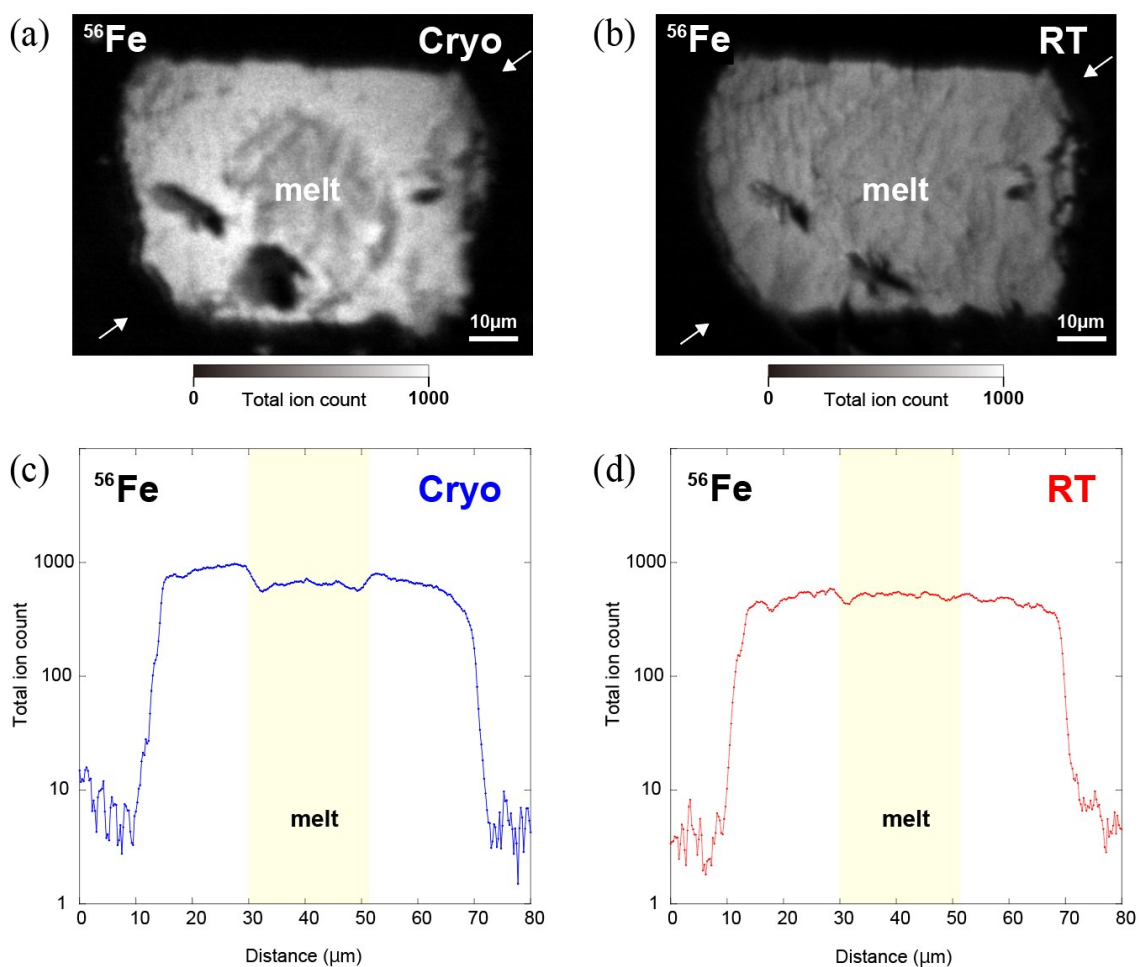
349



351

352 **FIGURE 2** | (a) Hydrogen image of an Fe foil analyzed using Cryo-SIMS, and (c) its line
 353 profile between the arrows. Hydrogen signals were detected from the center of the laser-heated
 354 hot spot (quenched melt) and from the rest of the Fe foil (unmelted). Hydrogen was also emitted
 355 from the edge of a Re gasket holding the sample. It shows the extent to which rhenium has
 356 hydrogenated, indicating that a limited amount of hydrogen was lost from a sample chamber
 357 to the gasket. The ratio of hydrogen signals from the unmelted Fe-H to liquid is approximately
 358 5:1. (b) After cryo-analysis, the sample temperature was temporarily raised to room
 359 temperature in a vacuum overnight, and Cryo-SIMS analysis was then performed again on the
 360 cryo-stage. A small amount of hydrogen was still emitted from the edge of the Re gasket and
 361 from the remaining KCl pressure medium, while the hydrogen signal from the Fe foil was
 362 below the noise level (negative counts resulted from dark frame subtraction) (d). The counts in
 363 (c) and (d) were obtained by subtracting the counts in a dark frame from those in a sample
 364 measurement.

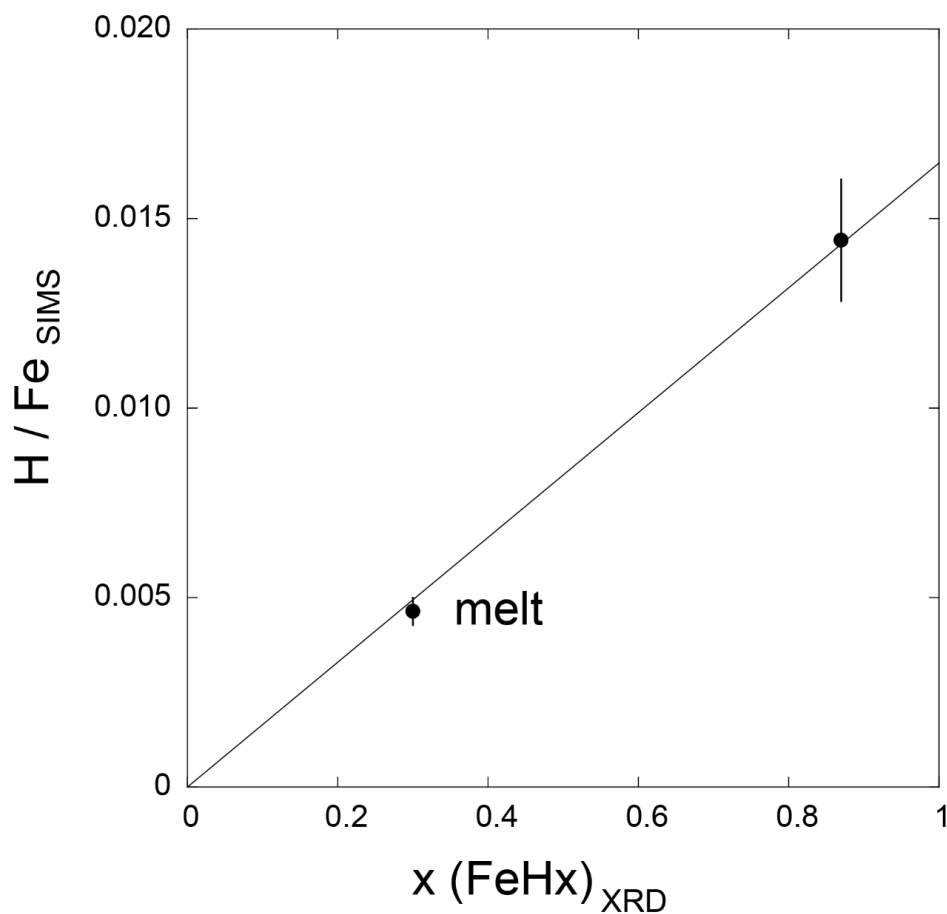
365



367

368 **FIGURE 3** | Iron maps collected with Cryo-SIMS before (a, c) and after the sample
 369 temperature was increased to room temperature temporarily and hydrogen was lost from iron
 370 (b, d). Similar to the hydrogen maps in Figure 2. The iron intensity in the melted area where
 371 hydrogen concentration has been reduced is lower than the surrounding area (a) and is further
 372 lowered after all hydrogen has been lost from the Fe foil (b). The iron intensity is thus positively
 373 correlated with the impurity (hydrogen) concentration, showing a matrix effect (the effect of
 374 the difference in crystal structure between before and after increasing the temperature to room
 375 temperature may be minor).

376



378

379 **FIGURE 4** | Comparison between the H/Fe count ratio obtained by Cryo-SIMS and hydrogen
380 concentration, x in FeH_x (equivalent to the H/Fe molar ratio) from XRD data for the melted
381 and unmelted areas in a sample. These data are plotted nearly on a straight line going to the
382 origin of the coordinate system, indicating that both measurements are consistent with each
383 other. This line may be used as a calibration curve for the SIMS determination of hydrogen in
384 iron.